Influence of the arrangement of multiple radiant ceiling panels on the radiant temperature field

Matthieu Labat, Sylvie Lorente, Mohamed Mosa

Influence of the arrangement of multiple radiant ceiling panels on the radiant temperature field

Matthieu Labat*, Sylvie Lorente, Mohamed Mosa

LMDC, INSA/UPS Génie Civil, 135 Avenue de Rangueil, 31077 Toulouse cedex 04 France.
*Corresponding author: m_labat@insa-toulouse.fr

Abstract

The use of radiant systems for cooling purposes in buildings is attracting considerable attention, particularly for Suspended Radiant Ceiling Panels (SRCPs). However, the arrangement of the panels on the ceiling and the influence on radiative heat transfer is rarely discussed in the literature. The objective of this paper is to provide a numerical study of the radiative heat transfer at room scale when the size and the number of SRCPs varies. It has been observed that the use of a single large panel would result in a low average temperature, which is desirable, but also in poor uniformity of the temperature field. Here, a genetic algorithm is proposed and tuned to determine the positions of multiple SRCPs that would improve uniformity. It is shown that much better uniformity can be obtained, with only a moderate increase in the average temperature, for 10 panels or more. The differences between the use of a single large panel and multiple panels is noteworthy when SRCPs cover from 10 to 70% of the ceiling area.

Keywords:

Suspended Radiant Ceiling Panels, Radiative cooling, Genetic algorithm, Heat transfer at room scale

Nomenclature:

Latin Symbols	Description	Unit
f	Fitness value	-
H	Distance between the ceiling and the working plane	m

G	Size of the grid for the ceiling	-
K	Size of the grid for the working plane	-
L	Length	m
N	Number of panels	-
R	Ratio	-
s	Standard deviation	
S	Surface	m^2
T	Temperature	K or °C
V	View factor	-
W	Width	m
Greek Symbols		
ε	Emissivity	-
λ	Number of children in a generation	-
μ	Number of individuals in a generation	-
σ	Stefan-Boltzmann constant	$5.67.10^{-8}$ $W.m^{-2}.K^{-4}$
ϕ	Heat flux	$W.m^{-2}$
Subscripts		
A	Absorbed	
C	Combination	
E	Emitted	
Env	Environment	
p	Probability	
P	Panel	
R	Radiant	
S	Shape	
Upper scripts		
$\sim$	Dimensionless	
$-$	Mean	

1. Introduction

A radiant system (RS) refers to a surface that exchanges heat with its surroundings mostly by radiation (at least 50% of the total heat transfer [1]). RS can be integrated into, embedded in or mounted on building structures (ceiling, floor, or walls) and accordingly categorized as thermally activated building systems (TABS), embedded radiant systems or Suspended Radiant Ceiling Panels

(SRCPs) [2]. Among the radiant systems, SRCPs present the specific advantages of being easy to integrate in the drop ceilings of existing or new buildings, thus offering more design flexibility, reconfiguration possibilities, and easy access for maintenance.

The popularity of radiant systems has been increasing in recent years. They are considered as a promising solution to improve the thermal comfort of buildings. This growing interest is due to several factors, including: high potential for energy savings, low level of noise, flexibility of design, and space savings [3,4]. This advantage can be mostly attributed to the fact that radiant systems rely mainly on radiation to transfer or receive heat from the conditioned zone, which influences the heat balance and comfort [5]. As a result, the amount of supplied the air is drastically reduced compared to classical all-air systems [4]. One of the consequences is that the noise created by the fans is strongly reduced [1,6]. Moreover, most RS operate with water because of its high thermal capacity, which results in a smaller quantity of fluid being required to flow and exchange heat with the conditioned space. Consequently, less energy is consumed. In contrast, conventional air systems utilize air as the thermal fluid to heat or cool a desired place by means of heat convection. As air has a lower thermal capacity than water, it has to be forced to flow in large volumes to create satisfactory comfort, so high power is required to operate these devices [7,8]. In addition to their potential for energy savings and quiet operation, RS can be considered as eco-friendly technology. RS run at low loads, which makes these systems compatible with renewable technology. Solar or geothermal energy can be coupled with these systems as renewable heat sources to efficiently supply warm or cold water over a suitable temperature range to improve thermal comfort [6,7]. Here, it should be observed that comfort is not only about heat transfer but also includes lighting and acoustics, the latter often being treated by means of systems placed on the celling. Therefore, there is less space for radiant systems to be installed and compromises have to be reached, as exemplified in [9], where the reduction of the surface emitting radiation was balanced by the use of fans in order to maintain the same heat flux. Another possibility is to consider perforated SRCPs equipped with sound absorbent

material [10]. A second major drawback of RS systems lies in the fact that the latent loads of the building, which still have to be removed by means of air renewal. A direct consequence is that the operative temperature of RS systems is limited by the dew point temperature.

SRCPs have been developed over many years and are now mature for building applications. Many studies (not reviewed here) have focused on the design and control of the SRCP itself, but heat transfer at room scale has been investigated less intensively. Nevertheless, some experimental set-ups have been built and tested. Some of them are briefly presented here. [11] analysed the global performance of SRCPs experimentally in a simulated hospital room (5.30 m long, 3.60 m wide and 3.0 m high). The test room was placed in a thermal chamber to control the thermal conditions of the surroundings. The room was equipped with SRCPs arranged in 3 rows in parallel, with 7 panels in series in each row, covering 13.86 m^2 of the ceiling surface (73%). The panels were installed at a height of 2.60 m. Each panel was 1.10 m long and 0.60 m wide. The results revealed that the SRCPs provided a cooling capacity ranging from 60.6 to 114.8 W/m^2. [12] conducted another study to evaluate the performance of SRCPs for a heating-cooling application. In this study, 4 SRCPs arranged in parallel were incorporated within the suspended ceiling to cover 63% of the surface area of a small room (14 m^2 ceiling area and 3.4 m height). The cooling capacity of the panel varied from 30 to 60 W/m^2. The thermal comfort conditions in an occupied room with various internal loads was modelled and simulated during cooling via a radiant ceiling by [13]. A well-insulated test chamber equipped with a radiant cooling surface symmetrically positioned on the ceiling and covering 56% of the available area was the subject of this study. [14] carried out several experiments to compare the thermal comfort conditions of a radiant ceiling panel and a convective system for a small meeting room. Radiant panels were attached to the roof at a height of 2.70 m, using 56% of the surface area (of 33 m^2) for heat exchange with the test room. A 55 m^2, full scale, laboratory experiment in a typical US office configuration was presented by [15]. The experimental facility included two rows of five windows on the southern façade. Six work spaces were simulated by means of thermal

manikins, computers and desks, together with ceiling fans, artificial lights and a sprinkler on the ceiling. Seventy-two SRCPs were arranged over the ceiling, covering almost 50% of its area. The arrangement was not uniform, yet not discussed. The thermal stratification during SRCP operation for cooling was found to be insignificant. Slight discomfort was measured close to the windows, but it was claimed that this could be mitigated by interior or exterior blinds and that a special design of the hydronic loop would be unnecessary. At a larger scale and in a real building, SRCPs were installed in two rooms having floor areas of 104 and 174 m^2, so that the SRCPs covered 45 and 40% of the ceilings, respectively [16]. The measured heat fluxes were found to meet the theoretical values.

The geometry of the room and of the panels are compared in Table 1 for the 6 experimental set-ups reviewed. It can be observed that the number and size of the panels may vary significantly. It is also notable that the distribution of the SRCPs on the ceiling was not discussed, even though it may have an influence, as 27 to 60% of the ceiling was not occupied by SRCPs.

Table 1 : Synthesis of the configurations reviewed in the literature

Reference	Floor area m^2	Area of a single panel (m^2)	Number of panels	Covering
[11]	19	0.66	21	73%
[12]	14	2.2	4	63%
[13]	15	8.4	1	56%
[14]	33	1.85	10	56%
[15]	55.7	0.372	72	48%
[16]	104	1.26	37	45%
	174		55	40%

Up to now, SRCPs have often been designed using one or multiple pipes placed just above a highly conductive plate, as illustrated in Fig.1. A pump forces cold water through the pipe at a given flow rate $\dot{m}$. Depending on the application, warm or cooled water is supplied to the panel from a hydraulic network to control the temperature of the thin sheet that exchanges heat with the surrounding surfaces. The temperature at the inlet cannot be lower than the dew point temperature, which limits

the cooling power somewhat. To maximize the cooling power, the mass flow rate is increased to such an extent that the temperature of the water does not vary much between the inlet and the outlet of the system. As things stand, SRCPs have to be connected to a water distribution system. Even though it is theoretically feasible to build complex networks in order to provide water for any panel arrangement, it seems obvious to test basic arrangements first for the sake of simplicity. More recently, however, another technique has been used to remove heat from an SRCP without using a cooling fluid: it relies on thermoelectric devices as exemplified in [17,18]. In the latter study, cooling units were sized down to 0.1 x 0.1 m^2 panels, and densities of radiant panels ranging from 9 to 25 per square meter were considered. Such systems enabled panels to be designed and arranged in a more complex fashion than with the hydraulic technique.

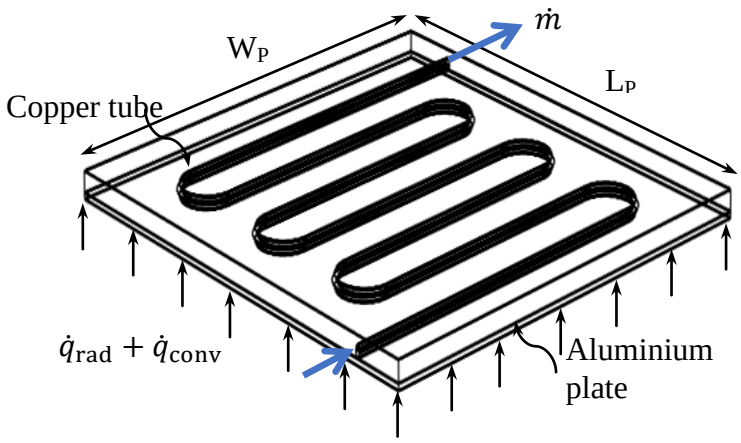

Fig.1: Scheme of a typical SRCP system made of a copper tube placed above an aluminium plate (adapted from [19])

To sum up, the use of radiant systems, particularly SRCPs, is attracting attention for cooling purposes in buildings. Most of the studies reviewed focused mainly on the system itself, rather than on the radiative field at the room scale. By this, we mean that SRCPs are used to provide a cooling power first. Even though a high fraction of heat is transmitted by radiation, the radiant temperature field at the room scale cannot be easily predicted because of the non-linear behaviour of radiative heat transfer and complex 3D configurations. Therefore, it is suspected that the radiant temperature field is pushed aside at the design stage when SRCP are considered for an application at the room

scale, while the heat balance at the room scale can be investigated more certainly. However, the distribution of the SRCPs has certainly an impact on the radiant temperature field and deserves attention. As it is rarely discussed in the literature, we propose to focus on this aspect by providing an extensive analysis at the room scale. Second, we decided not to focus on specific room and panel dimensions in order to be as general as possible and to explore a high number of possible distributions, which is relevant with the advent of thermoelectric devices. This work does not intend to provide some guidelines in the arrangement of SRCPs in a real environment, but highlights to what extent the distribution may have an influence on the radiant temperature field.

The next section presents the methodology and, more specifically, introduces the use of a Genetic Algorithm (GA) to search for the SRCP distribution that provides the most comfortable indoor conditions. The GA will be carefully validated step by step in order to give confidence in the results. Finally, the results will be presented in the third section.

2. Methodology

2.1. Statement of the problem

We consider a rectangular room with a floor area of (L x W) m^2, equipped with one SRCP, of dimensions (W_P x L_P) m^2, on its ceiling. The objective is to compute the heat transferred from the SRCP to a plane surface located at a distance H from the ceiling. Its area is the same as that of the ceiling and will be referred to below as the working plane (see Fig.2). The working plane is typically located 1 m above the floor in offices. For the sake of simplicity, no other architectural elements (doors, windows, post and beams, shelves, etc.) are considered.

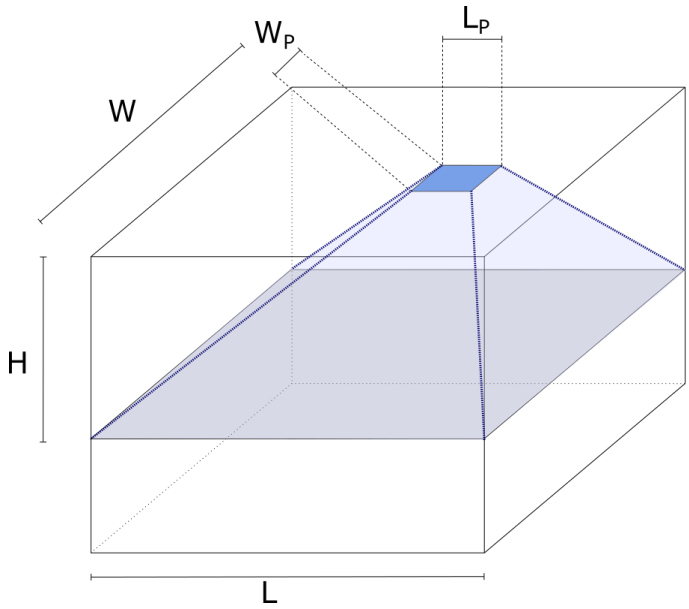

Fig.2: Room equipped with a single SRCP emitting radiation toward the working plane

In order to compare different cases, we propose to define two non-dimensional ratios. First, R_S is defined as in (1) so as to represent the shape of the room. W is defined to be always shorter than or equal to L, meaning that a square room is considered when R_S equals one, and a rectangular room when R_S is less than one.

$$R_S = \frac{W}{L} \tag{1}$$

Next, R_P is defined so that it represents the ratio of the SRCP area to the ceiling area. When R_P equals one, the ceiling is entirely covered with SRCPs.

$$R_P = \frac{W_P \cdot L_P}{W \cdot L} \tag{2}$$

Adapting equation (2) to the case where N panels are used instead of only one, we obtain:

$$N \cdot W_P \cdot L_P = R_P \cdot W \cdot L \tag{3}$$

In order not to focus on a specific shape of panels, we simply assume that the shape of the panel is identical to that of the room (so R_S is identical for room and panels). It is acknowledged that this assumption consists in a limitation in terms of application. Nevertheless, it also gives freedom for

exploring the influence of the number of panels. Also, we obtain the following constraints on panel dimensions (L_P and W_p) for an arrangement of N panels.

$$L_P = L \cdot \sqrt{\frac{R_P}{N}}$$
$$W_P = W \cdot \sqrt{\frac{R_P}{N}} \quad \textbf{(4)}$$

To determine the position of the panel on the ceiling, we propose to define a number of fixed positions in the form of a grid. Because of the above mentioned constraints, it is a G x G grid, where G is the integer part of a square root, as presented in (5). Note that this kind of grid is similar to the suspended ceilings commonly used in offices.

$$G = \left\lfloor \sqrt{\frac{N}{R_P}} \right\rfloor \quad \textbf{(5)}$$

As illustrated in Fig.3, the size of the grid does not match the size of the ceiling exactly for most of the values of N and R_P. Here, it was decided to place the grid at the centre of the ceiling, so that the SRCPs would not be positioned on the edges. Note that the edges correspond to the worst case scenario in terms of radiative heat transfer with the working plane, because a large part of the radiation would be absorbed by the adjacent vertical wall instead of the working plane.

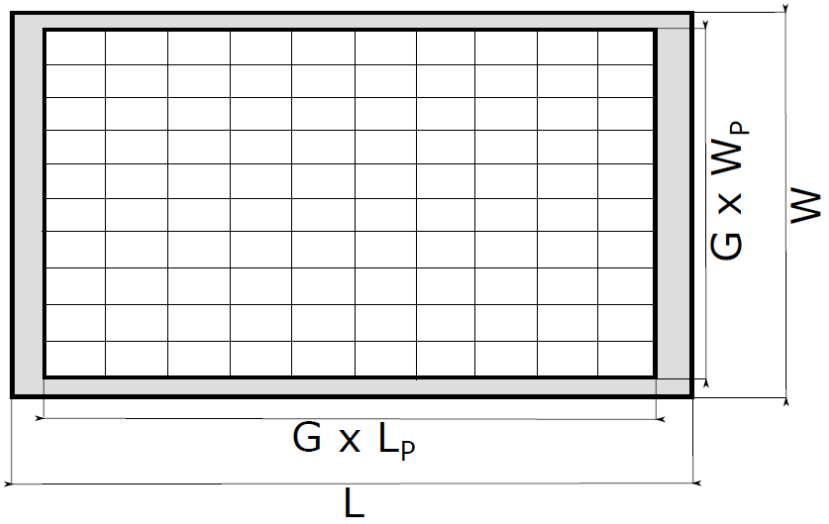

Fig.3: Example of grid obtained for G = 10

For N panels to be positioned in this grid, the number of possible combinations, N_C, is given by (6).

$$N_C = \frac{G^2!}{(G^2 - N)! \cdot N!} \quad \textbf{(6)}$$

For example, N_C equals 2300 for N = 3 and R_P = 0.1 (which corresponds to the use of 1.33 m² panels in a 40 m² room). But if N is increased to 10 (using 0.4 m² panels), the number of possible combinations reaches 1.7 10^{13}. Note that, for identical wall temperatures, the problem exhibits axes of symmetry. Consequently, several different distributions of SRCPs would lead to the exactly the same result, reducing the number of possible combinations.

This methodology introduces a limit for high R_P and low N values, as G^2 approaches N. In practical terms, it means that very few (or even no) elements of the grid contain zero panels. The sides of the ceiling, outside the grid and coloured grey in Fig.3, account for a fraction of the ceiling close to (1-R_P). For example, considering N = 20 and R_P = 0.7 leads to 5 elements with no panels, while there are 16 for R_P = 0.5. Even though N_c remains high in both situations (>10^{20}), it can be observed that R_P higher than 0.7 is more representative of an entire ceiling being radiative, with some parts being obstructed by other elements (acoustic panels, lighting systems). For this reason, the present study is limited to cases where R_P is lower than 0.7.

2.2. Radiative heat transfer at room scale

In this study, we focus on radiative heat transfer in a room equipped with SRCPs. Convective heat transfer is not considered here. Two reasons justify this assumption. First, as mentioned in the introduction, one of the main advantages of SRCPs is to provide comfort by removing heat by radiation, the latter being a function of surface temperature only. It is acknowledged that convection influences the energy balance of the SRCP. However, SRCPs are generally temperature controlled because of the risk of condensation, and the heat flux is a consequence. Therefore, the radiative heat flux should not be significantly influenced by convection. Second, convective heat transfer is significantly influenced by the use of the ventilation system (or by air movement in a naturally ventilated building), resulting in complex situations that are case specific and would lead to much more intensive computational work.

To describe radiative heat transfer, we define and calculate a temperature that represents the thermal environment, the latter being easier to interpret than a heat flux. Here, this temperature will be referred to as the perceived radiant temperature and will be denoted T_R. It should be mentioned that T_R differs from the radiant temperature as defined in [5], which is a standard dedicated to the estimation of indoor comfort. Generally, the radiant temperature is measured with a device called a "black globe", which integrates the radiative fluxes from all directions equally. It is evident that, for an identical environment, considering a flat surface oriented toward the ceiling instead of a sphere at the same position does not lead to the same result. However, flat devices are also used for assessing comfort, especially under asymmetric radiative conditions when a heating floor is used for example. A plane pyranometer was used in [20] to measure the radiative flux emitted by halogen lamps and define its impact on local skin temperature and thermal comfort. Overall, it is acknowledged that advanced techniques exist to evaluate indoor comfort and the influence of thermal radiation. However, the objective of the present study is not to precisely evaluate comfort but to determine the influence of the position of SRCPs on the temperature field. In this situation, considering a flat

surface oriented toward the ceiling for the computation of the perceived radiant temperature is justified.

The radiative heat flux emitted by an SRCP is a function of its temperature T_P. Note that, in the literature, a rather homogeneous temperature (± 1°C) is generally obtained over the surface of an SRCP. For hydraulic systems, different pipe to plate assemblies have been tested in order to minimize the temperature difference over the plate [21]. This indicates that achieving a uniform temperature distribution over the whole area of an SRCP is included in the design process. Therefore, it is reasonable to assume that the heat flux emitted from an SRCP can be modelled by considering a single value for its temperature. Both the emitting and absorbing surfaces were assumed to behave as black bodies. This strong simplification was used to stress radiative heat transfer. It is acknowledged that construction materials are grey bodies, meaning that reflected radiation should be included. However, the emissivity of construction materials is generally high [22], meaning that the assumption of black bodies is acceptable.

$$\phi_E = S_E \, \sigma \, T_P^4 \tag{7}$$

The working plane is discretized in a K x K uniform grid. Here K is set to 100, so that 10^4 values of the heat flux received by the working plane are computed. For each of the j elements of this grid, the absorbed heat flux is given by (8), where $V_{i \to j}$ is the view factor, which represents the proportion of radiation leaving surface i and striking surface j, and M represents the number of areas visible from j.

$$\phi_{A,j} = \sum_{i=1}^{M} V_{i \to j} \, \phi_{E,i} \tag{8}$$

The analytical expression of the view factors used in this problem was obtained from [23] and was implemented in Matlab. Note that the calculation differs for surfaces located in parallel or perpendicular planes (see Appendix). The analytical expression of the view factors was used here

because of its simplicity, while it is acknowledged that advanced techniques are necessary to deal with complex 3D geometries, as exemplified in [24].

In the present study, only two different surface temperatures are considered: the one of the *N* SRCPs, denoted T_P, and all the remaining ones, denoted T_{Env}. Therefore, the heat flux received by one element of the working plane can be written:

$$\phi_{A,j} = \phi_{E,T_{Env}} \sum_{i=1}^{M-N} V_{i_{T_{Env}} \rightarrow j} + \phi_{E,T_p} \sum_{i=1}^{N} V_{i_{T_P} \rightarrow j} \quad \textbf{(9)}$$

A numerical test was implemented within the code to systematically verify that the sum of the view factors was equal to 1 for every *j* element, with a tolerance of 10^{-10}.

Finally, the perceived radiant temperature $T_{R,j}$ is defined based on the absorbed heat flux for one element of the working plane, as follows:

$$T_{R,j} = \left(\frac{1}{\sigma}\phi_{A,j}\right)^{\frac{1}{4}} \quad \textbf{(10)}$$

This method allows the field of T_R to be computed all over the working plane for a given arrangement of SRCPs.

A comparison was performed with some of the experimental results provided in [25]. The latter study focused on a train berth equipped with a capillary radiant panel. The 1900x800 mm^2 panel was installed 900 mm above the mattress. The berth was surrounded with baffles made of 15 mm thick planks covered with a 20 mm thick insulation material. The surface temperature on the indoor sides of the baffles was monitored by means of T-type thermocouples, as long as the air temperature. The reported accuracy of these sensors is ±0.1°C. In this study, the authors present the Mean Radiant Temperature (MRT) as a function of time for given berth, aisle and panel temperatures. Although the calculation of the MRT differs from the methodology used for computing the perceived radiant

temperature, both indexes rely on the same definition and can be compared. One specific result was extracted from [25], where the MRT was found equal to 26.9°C for the upper face of the body, when the berth temperature and the panel temperature were measured at 24.2 and 33°C respectively. The temperature of the sixth face of the box, namely the curtain, was not mentioned explicitly. However, it was deduced that its temperature was close to 21.5°C, which is consistent with the measured temperature of the environment (20.5°C). These data were implemented in our code and the T_r value was equal to 27.28°C. Therefore, the discrepancy with the value provided by [25] is only 0.38°C, which remains acceptable considering the simplifications made here.

2.3. A brief description of genetic algorithms

As mentioned in section 2.1, as soon as the number of panels, N, increases, the number of possible combinations, $N_{C,}$ increases to such an extent that it prohibits the use of a comprehensive approach. This justifies the use of a non-systematic technique to discover the distribution of multiple SRCPs that favours radiative heat transfer.

Genetic algorithms (GA) are optimization techniques that have already been applied to a wide range of problems. In fact GAs group together different kinds of algorithms. Nevertheless, they all rely on a similar basis, as illustrated in Fig.4, which can be broken down as follows:

1. A generation of μ individuals is made, each one being characterized by its genome. The genome contains the variables, here the positions of the SRCPs, that have to be determined in order to find the optimal solution. The first generation is generated randomly.
2. The performance of each individual is evaluated through a mathematical model. In this paper, it is the computation of the perceived radiant temperature on the working plane. The objective is to rank the individuals, meaning that their performances have to be defined through a limited number of values, named fitness values.

3. Some of the individuals are selected among the generation in order to perform cross-over. The selection is defined so as to favour the individuals with the best fitness values. Cross-over defines a set of λ new individuals (named "children") from the ones that were selected (named "parents"). More precisely, the genomes of the children are based on those of their parents. Next, some of the children are randomly selected to be mutated, meaning that a fraction of their genome is modified again, independently of the genomes of the parents. Finally, the fitness values of all the children are evaluated by using the same mathematical model as before.
4. A new generation is defined, which may contain only a fraction of the children, or a combination of the parents and the children (when such a technique is used, it is referred as elitism). The technique used for this step is often called evolution strategy.
5. If the stopping criterion has been reached, the algorithm stops and the latest generation is kept. Otherwise, the latest generation is taken as parents for the algorithm to repeat from step 3. The stopping criterion is defined in such a way that it is reached when the optimal fitness value has been obtained with confidence.

Overall, GA combines some techniques used to converge toward the optimal fitness value (selection, cross-over, elitism) and steps used to explore the research space (random generation, mutation). Depending on the fitness landscape, some techniques (or evolution strategies) are preferred over others to obtain the optimum fitness value faster and with confidence. This can be illustrated through the use of some specific mathematical functions to test the algorithm (Rosenbrock's, Rastringin's or Himmelbau's function). The interested reader is invited to refer to [26] for a broader description of GA, or to [27] for evolution strategies.

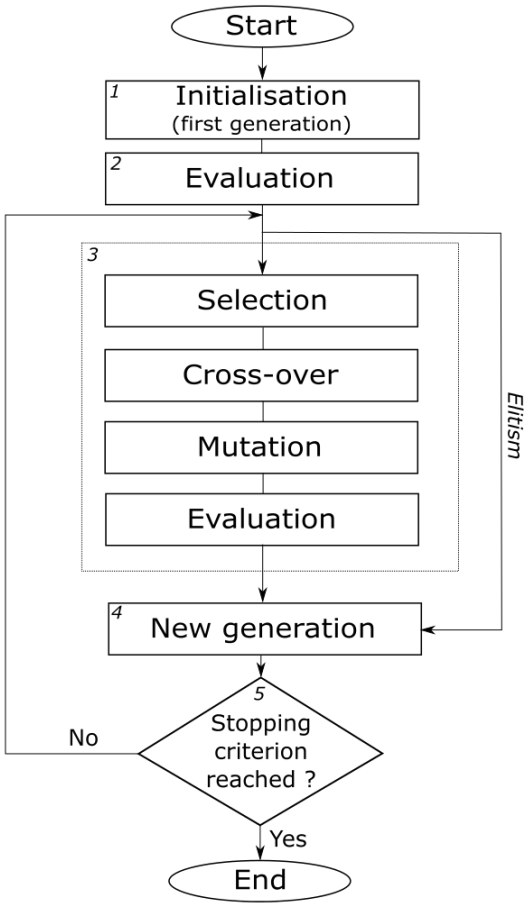

Fig.4: Flow chart of a generic genetic algorithm

In [28], studies dealing with GA techniques applied to heat transfer problem have been reviewed. Overall, they suggest not to describe extensively the GA procedure, as it can be considered as mature now, but the tuning of the evolution strategy and the repeatability of the GA (i.e., the fact that two runs with the same settings can lead to different results) should be considered carefully. It was shown that this technique performs well for a wide range of problems, from design optimization to inverse heat transfer problems or heat transfer correlation. An example similar to the problem treated here can be found in [29], where they aimed to optimize the shape of a radiant enclosure by minimizing the thermal resistance between the surfaces of the enclosure. The problem was solved numerically using a Genetic Algorithm (GA) implemented in Matlab. Also in the context of radiant enclosure, [24] studied the uniform thermal conditions produced by panel heater on the surfaces of 3-D design

object. A genetic algorithm was used to obtain a uniform heat flux distribution on the surface of the object.

In the present study, the genome of an individual is defined to contain the position of all the panels over the ceiling. This introduces constraints on the handling of the GA, as the different parts of the genome are not independent. As the objective is to look for the position of N panels that improves the perceived radiant temperature; two panels cannot have the same position. Moreover, the cross-over and mutation operators have to be designed in order to allow both convergence and exploration. This is hardly feasible if the genome is structured (for example by sorting the positions of the panels). For example, a panel located in the middle of the ceiling should be used to perform cross-over with another one located in a corner. On the one hand, using a simple permutation operator for cross-over means that some positions of the ceiling would hardly be reachable, which would make the search for the best fitness values more difficult. On the other hand, using the general BLX-α technique means that the resulting position could be that of another panel, implying that the number of panels simulated on the ceiling may decrease, which is not acceptable. A similar risk arises for mutation. Consequently, the constraints on both the cross-over and mutation operators are significant. This led to the choice to develop a GA by using the Matlab environment rather than using some commercial tools, in which it is not feasible to introduce such constraints on the operators. However, the drawback associated with this choice is that the efficiency of the GA has to be demonstrated.

In the present work, rather simple, common techniques were used at first and were progressively tuned. This will be summarized in Section 2.5. It is acknowledged that more refined approaches are available today but our objective is not to propose an exhaustive test of the different evolution strategies. The technique was used here to determine whether the distribution of the SRCPs has a significant effect on the perceived radiant temperature field.

In next section, the influence of a single panel located in the middle of the ceiling is presented first, as it does not rely on the use of a GA. Second, the GA is presented and tuned by using the results obtained with a single panel.

2.4. Single panel placed in the middle of the ceiling

To illustrate the results obtained from equations (9) and (10), a single case was defined. Here, the area for the ceiling was fixed at 40 m^2, which is slightly higher than values used in the literature for prototype testing but more representative of a small office room (see Table 1). The distance between the ceiling and the working plane H was set to 1.5 m. A single SRCP was placed in the middle of the ceiling: it was assumed that most of the radiation emitted by the SRCP would be received by the working plane in this case. Therefore, this position favours heat transfer to the working plane. The area of the panel was defined such that R_P was 0.3. We recall that the dimensions of the panel were selected so that its R_S equalled that of the room, as proposed before. For this example, R_S was set to one.

T_{Env} was set at 25 °C, which is representative of indoor conditions when cooling is desired, and T_P was set at 15 °C. A lower value is hardly ever found in the literature because of the risk of water vapour condensation, which would result in liquid water dropping onto the floor and occupants. 15°C stands as the dew point temperature for indoor air at 21°C and 68% relative humidity, or 24°C and 56% relative humidity. It is acknowledged that the value for T_P should be selected depending on the climatic conditions and the indoor latent loads. Here it would fit for a rather dry climate.

The temperature of the vertical wall was assumed to be uniform and set at $T_{Env.}$ The results are presented in Fig.5, where only the contours of $T_{R,j}$ are plotted. The x and y axis, denoted $\tilde{L}$ and $\widetilde{W}$, corresponds to the dimensionless coordinates of the working plane. Note the non-homogeneous distribution of T_{Rj}, ranging from approximately 19 °C to 24.5 °C.

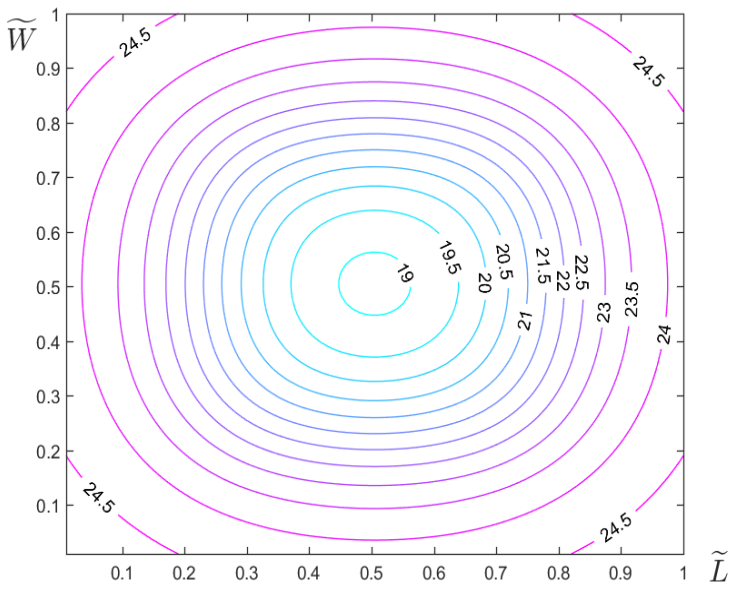

Fig.5 : Contours of $T_{R,j}$ on the working plane for a single panel (R_S = 1, R_P = 0.3, H = 1.5 m)

This case was computed repeatedly for R_P ranging from 0.05 to 0.7 and for R_S ranging from 0.25 to 1. Also, the computational work was repeated for H = 1.5 m and 3 m, so that it covers a wide range of ceiling and working plane heights. In the end, this led to a calculation of the temperature field for 608 different configurations. For validation purposes, the numerical work was repeated for every configuration by using the same values for T_{Env} T_P, which leads theoretically to a uniform temperature field for the working plane, whatever the values of R_P, R_S and H. The scattering of the computed temperature field remained lower than 7 10^{-9} °C for every configuration.

Both the mean value $\overline{T}_r$ and the standard deviation s of the temperature field were computed and used to plot Fig.6 and Fig.7, respectively. The standard deviation represents the spread of the temperature field: a low value indicates that the field is rather homogeneous (or uniform) over the working plane. As SRCPs are mainly used to provide indoor comfort, it was assumed that a uniform temperature field was more desirable.

First, $\overline{T}_r$ was found to have almost no impact for R_S higher than 0.5, and its influence remained slight for lower values. Therefore, the rest of the study focuses mostly on the influence of R_P and a square room is considered (R_S =1). This is in line with the results obtained by [29] where it was found that

the maximum heat flux (minimum thermal resistance) obtained when the aspect ratio of the enclosure R_S approaches 1.

Second, despite the nonlinear aspect of radiative heat transfer, the mean value of the temperature field was found to decrease almost linearly with R_P, especially for high R_S values. Also, the influence of H was highlighted. For a higher ceiling, the influence of the SRCPs was lower, leading to higher values of $\overline{T_r}$. Note that the conclusions on the influence of R_P and R_S were the same for both values of H tested here.

On the other hand, the computed standard deviation s (see Fig.7) exhibited more complex trends. It was observed that s increased strongly for R_P ranging from 0.05 to 0.3, the maximum value being reached when R_P was near 0.5. Finally, much lower values were obtained when the height of the ceiling was increased.

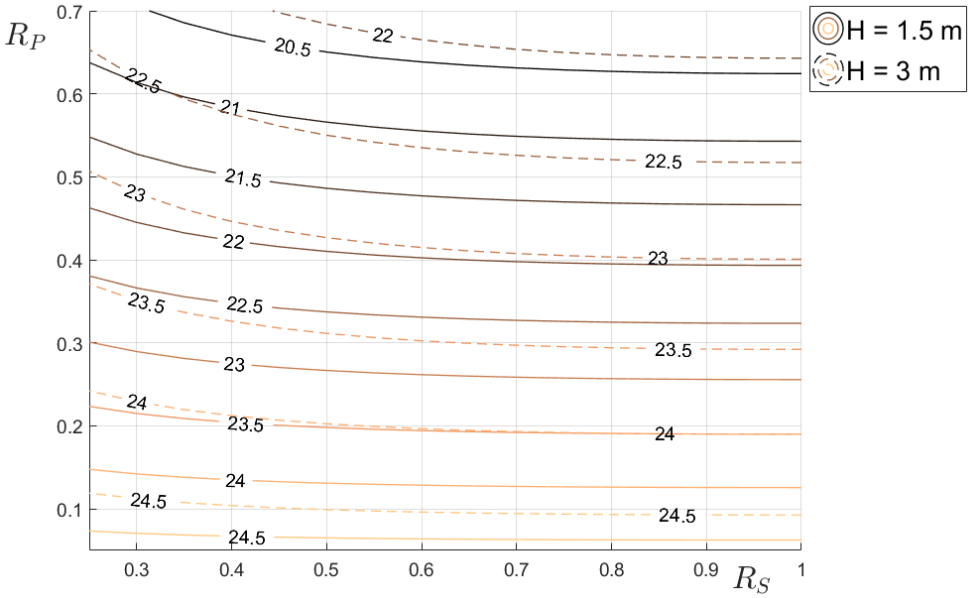

Fig.6: Contours of $\overline{T_r}$ (in °C) according to R_S and R_P for two values of H (full lines: 1.5 m; dashed lines: 3 m)

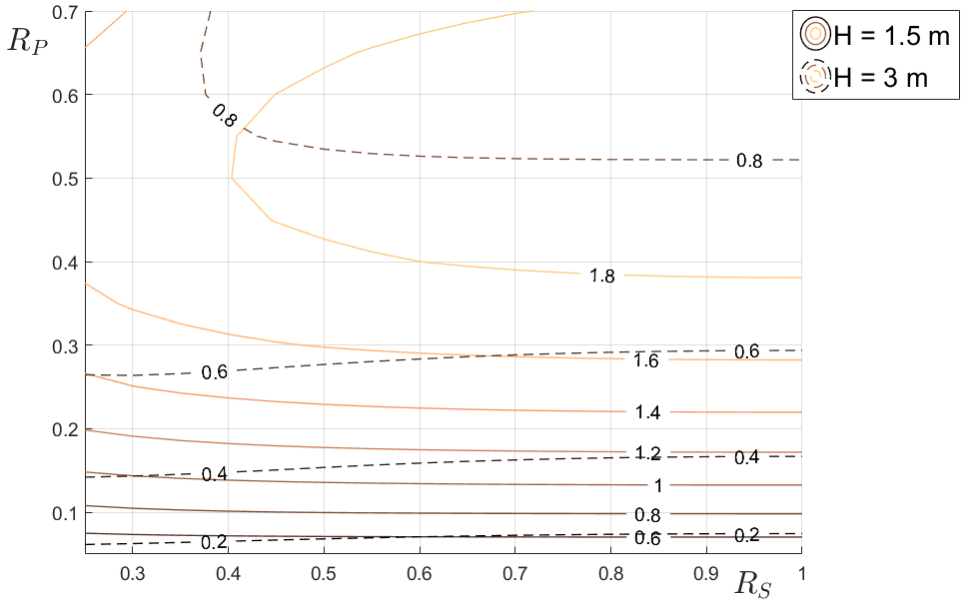

Fig.7: Contours of *s* (in °C) according to R_S and R_P for two values of H (full lines: 1.5 m; dashed lines: 3 m)

To sum up, the shape of the room is of little influence for this case, which is representative of a small office. The mean perceived radiant temperature can be roughly approximated as a linear function of R_P, but the uniformity cannot. Therefore, the latter is worth studying.

Also, as the shape of the panels was defined according to the shape of the room, the results may be more influenced by the ceiling height rather than the floor area. The difference would result from the ratio of ceiling area to vertical walls area, which is also influenced by the ceiling height. It is acknowledged that the mean perceived radiant temperature would be influenced but the impact on the distribution should remain equivalent. Therefore, a single value for the floor area (40 m^2) and *H* (1.5 m) is considered for the rest of this study.

2.5. Genetic algorithm tuning

This section gives a very brief description of the technical settings for the GA. Then a few parameters are tested in order to assess the repeatability of the GA, and finally a comparison with the results obtained with a single panel is presented.

A Latin Hypercube Sampling (LHS) algorithm was used to initialize the first generation. For selection, the stochastic tournament technique was selected. Three individuals were taken from the generation of the parents by using random sampling without replacement, one of the individuals being kept for cross-over. Cross-over was achieved by using the rather common blend operator (BLX-α): one element of the genome of the children (e.g. the position of one panel) is randomly chosen on a straight line defined by the two panels randomly taken from the two parents. Two parents were allowed to generate two children. A fixed 0.1 mutation rate was set and 20% of the genome of the selected children was modified randomly. No evolution strategy was used for the mutation parameters. The new generation was set using an elitist (μ+λ) evolution strategy. The cost function f_1 was defined so that it represented the mean perceived radiant temperature (see (10)) over the working plane. The objective of the GA was to define the positions of the panels on the ceiling for which f_1 was minimal. This choice was made for validation purposes, as we assume that the best distribution would be obtained when the panels are located in the middle of the room.

$$f_1 = \frac{1}{K^2} \sum_{j=1}^{K^2} T_{R,j} \qquad \textbf{(11)}$$

The stopping criterion was set so that the *f* value of at least 90% of the population was within 0.1% of the *f* value of the best individual. Also, the best individual had to remain the same for at least 5 generations. These techniques are quite common, and their tuning was achieved during early tests, not presented here.

As mentioned in [28], repeatability is crucial for GA and has to be assessed. Moreover, it is also known that μ greatly affects the efficiency of the GA. Therefore, one case was selected to be run 30 times, and this was repeated for different values of μ. This case was selected in such a way that the number of possible combinations, *Nc*, was high, making the test more demanding. The results (i.e., the minimal perceived radiant temperature for the latest generation) obtained for 30 runs were

averaged and are plotted against μ in Fig.8. It was observed that the stopping criterion was reached for 20 to 30 generations, regardless of the value of μ. The best and worst results among the 30 runs have been added to the figure to illustrate the discrepancy between several runs. It was found that the average value of $\overline{T_r}$ did not change much when the size of the population was greater than 25. The difference between the best and the worst run was 0.034 °C, which is insignificant with respect to the sensitivity of a human being to temperature. Finally, the computational time was found to increase linearly with μ. For 25 individuals, one run took approximately 150 s on a laptop using a 2.6 GHz Intel processor and 8Go of RAM, which is acceptable.

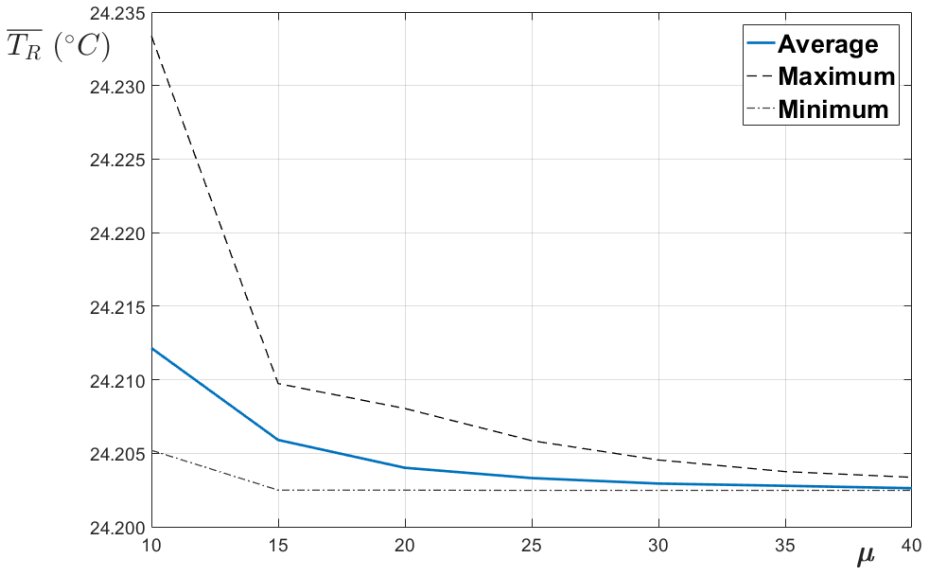

Fig.8: Results of the repeatability test for different values of μ (R_S = 1, R_P = 0.1 and N = 20)

A second test was carried out in order to compare the results obtained with the GA to the ones obtained in section 2.4. This test was run for N ranging from 10 to 30 and for R_P ranging from 0.1 to 0.7. The results are presented in Fig.9.

First, the GA was found to perform efficiently as the results were very close to the ones obtained for a single panel. This also confirms the assumption that the lowest temperature for a given value of R_P is obtained for a single panel placed in the middle of the room. Using multiple smaller panels, the total area being the same, will not lead to a lower mean radiant temperature. The difference observed in increased with increasing R_P and decreased with increasing N, although it always remained

smaller than 0.2 °C. The reason why a perfect match was never obtained is that the meshing of the ceiling depends on the number of panels (see equation (5)) and makes it impossible to obtain exactly the same geometry as for a single panel. Therefore, the observed difference resulted from methodological aspects, and not from the tuning of the GA. This indicates that the GA presented here is suitable to solve the problem.

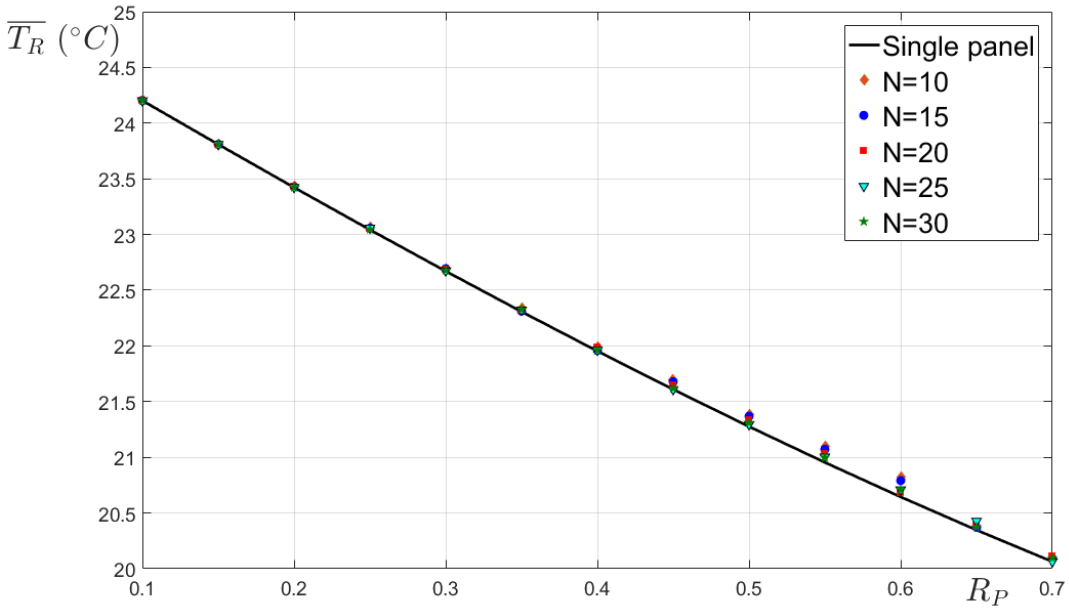

Fig.9: Best $\overline{T_R}$ values obtained for *N* panels and for a single panel placed in the middle of the ceiling (R_S = 1)

3. Results

3.1. Distribution of N panels for optimised uniformity

Once the robustness of the GA had been proved, it could be used to search for an efficient distribution of multiple SRCPs. As mentioned before, a lower mean radiant temperature cannot be obtained. However, the uniformity of the temperature field over the working plane can be improved. Therefore, a new cost function, f_2, was defined as shown in (12), based on the definition of the standard deviation *s*.

$$f_2 = \sqrt{\frac{\sum_{j=1}^{K^2}\left(T_{R,j} - \overline{T_R}\right)^2}{K^2}} \qquad \textbf{(12)}$$

As the problem to be optimized was slightly different, the tuning of the GA was tested again. Here, the repeatability was tested for the same case as before, but the cost function defined in (12) was used. Stable results were obtained for μ = 45. The average value of f_2 was computed on the basis of 30 runs and reached 0.08 °C, while its standard deviation was about 0.01 °C. Finally, the number of generations needed for the stopping criterion to be satisfied was approximately doubled. Consequently, the computational time increased to the same extent.

Next, the GA was used for R_P ranging from 0.1 to 0.7 and for N ranging from 10 to 30. The results are presented in Fig.10, where one point represents the best standard deviation s obtained by the GA for given values of R_P and N. The mean temperature $\overline{T_R}$ was computed afterwards (it was not included in the fitness values). The results obtained with a single panel (see section 2.4) are also plotted in Fig.10 (black curve). Note that the R_P values are not mentioned on Fig.10. As the results were scattered, the readability would have deteriorated.

Fig.10 clearly shows that a more uniform radiant temperature field can be obtained from distributed panels compared to the use of a single panel. s decreased to approximately 0.1 °C for low R_P values, while the minimum was close to 0.8 °C for a single panel. It was observed that s increased along with R_P, but remained much lower than for a single panel. For R_P = 0.5, for example, s ranged from 0.5 to 0.8 °C for multiple panels, while it was near 1.9 °C for a single panel (note that it correpsonds to the highest standard deviation). It is a remarkable fact that increasing the number of panels above 10 did not lead to significant improvements, except for the highest values of R_P, where the methodology is less appropriate as already mentioned. This result is in agreement with the findings of [24]. However, a less desirable effect was that the perceived radiant temperature increased sligthly. This was because a more uniform field is obtained when the SRCPs are scattered over the

ceiling but, as they get closer to the sides, a higher fraction of the emitted radiation is received by the vertical walls instead of the working plane. However, the increase of $\overline{T_R}$ remained lower than 1 °C in all cases, which is low reagarding human perception.

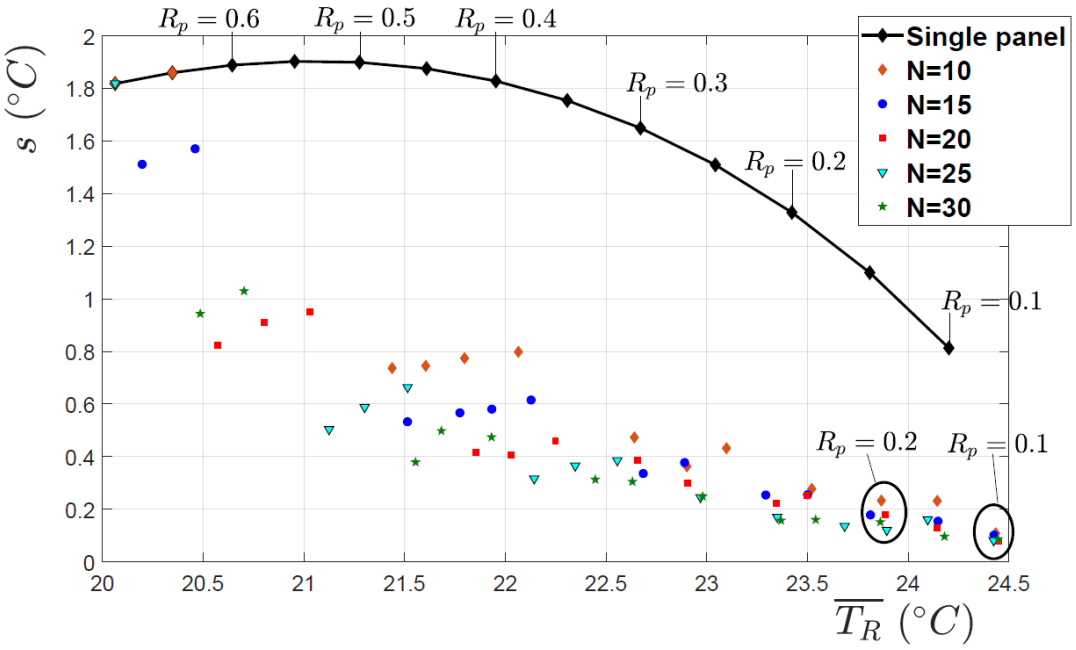

Fig.10: s and $\overline{T_R}$ values obtained for a single and multiple SRCPs when f_2 is used as the cost function (R_S = 1)

The perceived radiant temperature field is representative of indoor comfort, but is slightly different from the radiative heat flux because of the fourth power of the temperature (see (7)). The latter is often linearized in building physics because of the relatively low range of temperature commonly obtained in buildings. In order to provide a more comprehensive analysis, a third fitness function is defined in (13). It is similar to (12) but the standard deviation of the radiative heat flux is minimized instead of the temperature. This new metric is more representative of the energy balance on the working plane than indoor comfort.

$$f_3 = \sqrt{\frac{\sum_{j=1}^{K^2}\left(\Phi_{R,j} - \overline{\Phi_R}\right)^2}{K^2}} \qquad \textbf{(13)}$$

The results were analysed by means of two non-dimensional numbers, as defined in (14). For a given value of R_P, $\tilde{\phi}$ represents the relative decrease of the radiative heat flux received by the working plane because of the use of N panels instead of a single one located in the middle of the ceiling. $\tilde{s}$ represents the relative decrease of the standard deviation, under the same conditions. The results are presented in Fig.11. The best case would be obtained for $\tilde{s}$ = 1 and $\tilde{\phi}$ = 0.

$$\tilde{\phi} = \frac{\overline{\phi_R}|_{R_P,N} - \overline{\phi_R}|_{R_P,1}}{\overline{\phi_R}|_{R_P,1}}$$

$$\tilde{s} = \frac{s|_{R_P,1} - s|_{R_P,N}}{s|_{R_P,1}} \quad \textbf{(14)}$$

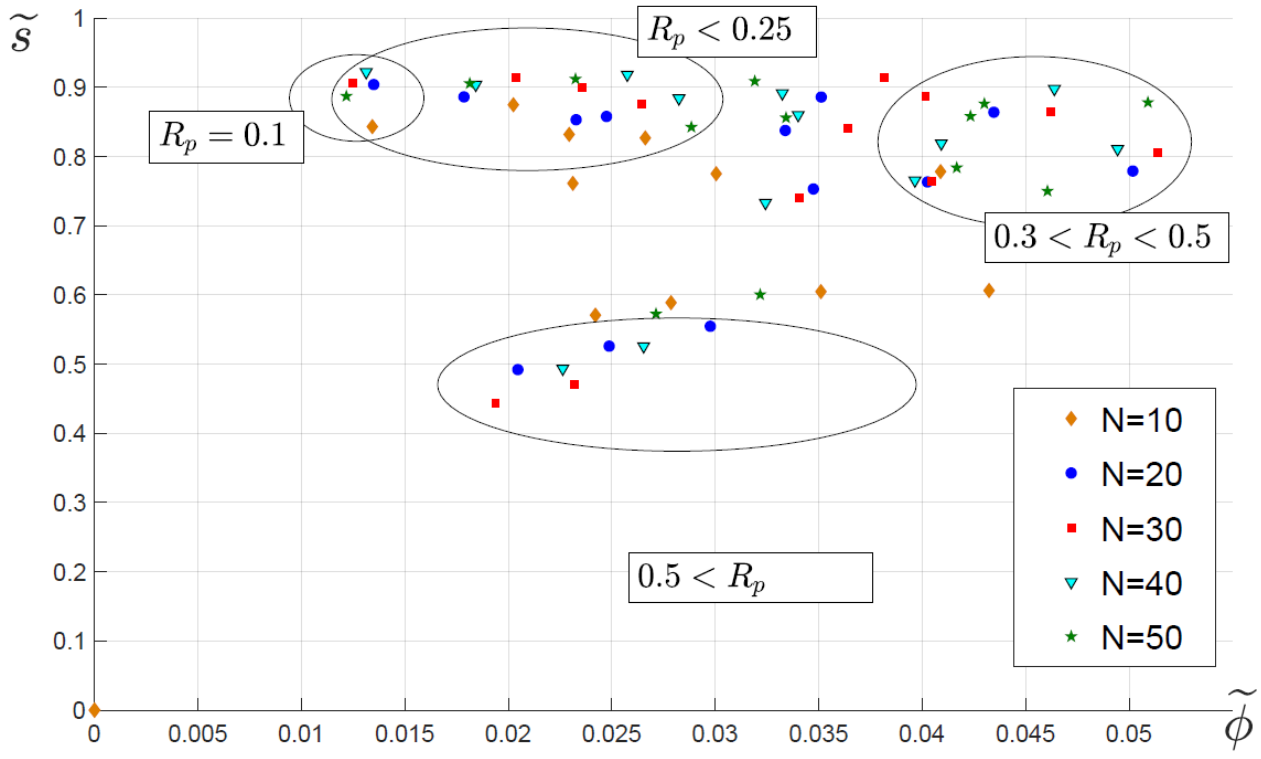

Fig.11: $\tilde{s}$ and $\tilde{\phi}$ obtained when f_3 is used as the cost function for R_P ranging from 0.1 to 0.7 (R_S = 1)

First, $\tilde{s}$ values higher than 0.5 were obtained most of the time, meaning that the uniformity can be twice as good with distributed panels as with a single one. The best results were obtained for the lowest values of R_P and were as high as 0.92. Even though the results were scattered, a trend could

be observed: $\tilde{s}$ decreased with R_P and dropped dramatically when R_P was higher than 0.5. This trend was less severe for 30 panels, however. The calculations were repeated for a large number of panels (up to 80). Similar trends were observed for R_P lower than 0.5 but, for higher values, the decrease of $\tilde{s}$ was less pronounced, as it remained between 0.5 and 0.6.

The maximum value for $\tilde{\phi}$ was rather low; the highest increase of the radiant heat flux was 5.3% and the average increase was 2.8%. These results confirm that a much better uniformity can be obtained with multiple panels instead of only one, without a significant increase of the radiant heat flux.

Finally, the probability density function (pdf) of the perceived radiant temperature is plotted in Fig.12 for one case only, for the purpose of illustration. The three different cost functions (see (11), (12) and (13)) were successively used to obtain the three pdfs.

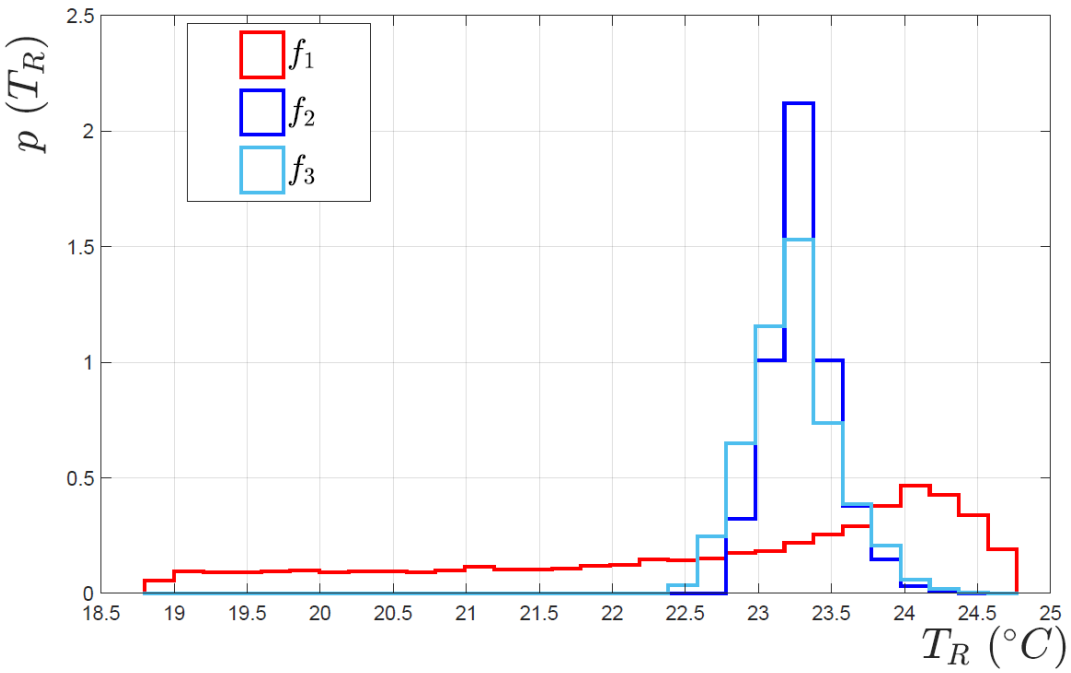

Fig.12: Probability density function of T_R obtained with the 3 different cost functions (R_P = 0.3; R_S = 1 and N = 25)

The pdf obtained when using f_1 as the cost function, which is equivalent to minimizing the mean perceived radiant temperature, is the same as the one obtained with a single panel. The pdfs obtained with f_2 and f_3 are the ones that improve the uniformity of the radiant temperature field and the

radiative heat flux, respectively. Note the narrower distribution compared to that obtained with f_1. Also, it can be observed that the differences between the results obtained with f_2 and f_3 are minimal, meaning that both approaches (considering the perceived radiant temperature or the heat flux) lead to similar results.

3.2. Limits and outlooks

This numerical work relies on several simplifying assumptions that are summarized here. First, only black bodies were considered, so that no reflected radiation was computed. Second, the geometry of the room was simplified: it does not include any architectural element and all the vertical walls were assumed to be at the same temperature. Finally, the SRCPs were assumed to be at a homogeneous temperature. Therefore, the results presented here cannot be applied directly to a practical case: a more refined modelling of the room would be required, so as the SRCPs. Also, the different temperatures should be set accordingly to a given climate and occupation. Still, the ranges in terms of mean value and uniformity of the radiant temperature field presented here should be of the same magnitude.

As illustrated in Fig.11, the problem is twofold, suggesting that a multi-objective optimization technique would be more relevant than a single objective technique. Multi-objective optimization algorithms allow a set of solutions (named the Pareto front) to be defined, for which one objective cannot be approached without moving away from another objective. A wide range of techniques exist, which perform differently depending on the problem to be optimized, as exemplified in [30]. In the present study, however, the radiative heat flux did not increase significantly when better uniformity was sought. Therefore, we assume that a multi-objective technique would not provide relevant improvements and that optimizing the uniformity only is satisfactory.

If a hydraulic network is used as a heat sink, the pressure loss is the parameter to be optimized. Optimizing its architecture for distributing the cold fluid to multiple panels also sounds challenging and could be considered for further work.

4. Conclusion

This paper investigates the influence of the distribution of multiple SRCPs on the field of radiant temperature for a plane surface facing the ceiling. The results are analysed through the mean value and the standard deviation of the temperature and radiative heat flux fields. It was observed that the use of a single panel would result in the lowest average temperature but also in poor uniformity. It was anticipated that better uniformity would be more desirable and could be achieved by using multiple panels instead of only one. The methodology proposed here relies on the discretization of the ceiling into a grid where N panels can be placed. Different cases were investigated according to the number of panels, the surface occupied by SRCPs on the ceiling, and the geometry of the room (but to a lesser extent). A genetic algorithm was proposed and tuned to determine the position of the SRCPs that led to the best uniformity. The results showed that uniformity could be significantly improved (the standard deviation was reduced by up to 90%) by using 10 panels or more. For the cases studied, increasing the number of panels did not lead to significant improvements. A notable drawback was that the mean radiant temperature increased. However, the heat flux received on the work plane increased by no more than 5%, which is negligible regarding the significant improvement in terms of uniformity.

Appendix – View factor calculation

For two rectangular areas, the general equation for view factor calculation is

$$V_{1\to 2} = \frac{1}{(x_M - x_m)\cdot(y_M - y_m)} \cdot \sum_{i,j,k,l=1}^{2} (-1)^{i+j+k+l} \cdot f(x_i, y_i, z_i, \alpha_i) \qquad \textbf{(15)}$$

For a horizontal rectangular area 1 (defined on $[x_1 : x_2]$ and $[y_1 : y_2]$) toward a vertical rectangular area 2 (defined on $[z_1 : z_2]$ and $[\alpha_1 : \alpha_2]$), where α and y are on the same axis,

$$f = \frac{1}{2\pi} \cdot \left[(y-\alpha)(x^2+z^2)^{1/2} \cdot atan(K) - \frac{1}{4}\left[(x^2+z^2)\cdot ln(1+K^2) - (y-\alpha)^2 \cdot ln\left(1+\frac{1}{A^2}\right)\right]\right] \qquad \textbf{(16)}$$

and

$$A = \frac{y-\alpha}{(x^2+z^2)^{1/2}} \qquad \textbf{(17)}$$

For a rectangular area 1 (defined on $[x_1 : x_2]$ and $[y_1 : y_2]$) toward a parallel rectangular area 2 (defined on $[\alpha_1 : \alpha_2]$ and $[\beta_1 : \beta_2]$), separated by a distance called h :

$$f = \frac{1}{2\pi} \cdot \left[(y-\beta)\cdot\sqrt{(x-\alpha)^2+h^2}\cdot atan\left(\frac{(y-\beta)}{\sqrt{(x-\alpha)^2+h^2}}\right) + (x-\alpha) \cdot\sqrt{(y-\beta)^2+h^2}\cdot atan\left(\frac{(x-\alpha)}{\sqrt{(y-\beta)^2+h^2}}\right) - \frac{h^2}{2} ln((x-\alpha)^2+(y-\beta)^2+h^2)\right] \qquad \textbf{(18)}$$

References

[1] ASHRAE, ASHRAE Handbook: HVAC systems and equipment., American Society of Heating, Refrigerating and Air-Conditioning Engineers, Atlanta, Ga., 2000.

[2] K.-N. Rhee, B.W. Olesen, K.W. Kim, Ten questions about radiant heating and cooling system[s], Build. Environ. (2016). https://doi.org/10.1016/j.buildenv.2016.11.030.

[3] H.E. Feustel, C. Stetiu, Hydronic radiant cooling—preliminary assessment, Energy Build. 22 (1995) 193–205.

[4] J. Niu, J. v. . Kooi, H. v. . Ree, Energy saving possibilities with cooled-ceiling systems, Energy Build. 23 (1995) 147–158.

[5] NF EN ISO 7730, Analytical determination and interpretation of thermal confort using calculation of the PMV and PPD indices and local thermal comfort criteria, (2006).

[6] K.W. Kim, B.W. Olesen, Radiant Heating and Cooling Systems. Part one, H R E J. 57 (2015) 28–37.

[7] K.-N. Rhee, K.W. Kim, A 50 year review of basic and applied research in radiant heating and cooling systems for the built environment, Build. Environ. 91 (2015) 166–190.

[8] B.A. Thornton, W. Wang, M.D. Lane, M.I. Rosenberg, B. Liu, Pacific Northwest National Laboratory, United States. Dept. of Energy, Technical support document 50% energy savings design technology packages for medium office buildings., Pacific Northwest National Laboratory, Richland, Wash., 2009. http://www.pnl.gov/main/publications/external/technical_reports/PNNL-19004.pdf (accessed November 7, 2016).

[9] C. Karmann, F. Bauman, P. Raftery, S. Schiavon, M. Koupriyanov, Effect of acoustical clouds coverage and air movement on radiant chilled ceiling cooling capacity, Energy Build. 158 (2018) 939–949. https://doi.org/10.1016/j.enbuild.2017.10.046.

[10] N. Fernandez, W. Wang, K.J. Alvine, S. Katipamula, Energy Savings Potential of Radiative Cooling Technologies, Pacific Northwest National Laboratory (PNNL), Richland, WA (US), 2015.

[11] N. Fonseca, Experimental study of thermal condition in a room with hydronic cooling radiant surfaces, Int. J. Refrig. 34 (2011) 686–695. https://doi.org/10.1016/j.ijrefrig.2010.12.019.

[12] J. Miriel, L. Serres, A. Trombe, Radiant ceiling panel heating–cooling systems: experimental and simulated study of the performances, thermal comfort and energy consumptions, Appl. Therm. Eng. 22 (2002) 1861–1873.

[13] V. Zmrhal, J. Hensen, F. Drkal, Modelling and simulation of a room with a radiant cooling ceiling, in: Proc Eighth Int. IBPSA Conf. Eindh. Neth., 2003.

[14] T. Imanari, T. Omori, K. Bogaki, Thermal comfort and energy consumption of the radiant ceiling panel system.: Comparison with the conventional all-air system, Energy Build. 30 (1999) 167–175.

[15] H. Jia, X. Pang, P. Haves, Experimentally-determined characteristics of radiant systems for office buildings, Appl. Energy. 221 (2018) 41–54. https://doi.org/10.1016/j.apenergy.2018.03.121.

[16] R. Li, T. Yoshidomi, R. Ooka, B.W. Olesen, Field evaluation of performance of radiant heating/cooling ceiling panel system, Energy Build. 86 (2015) 58–65. https://doi.org/10.1016/j.enbuild.2014.09.070.

[17] Y. Luo, L. Zhang, Z. Liu, J. Wu, Y. Zhang, Z. Wu, Three dimensional temperature field of thermoelectric radiant panel system: Analytical modeling and experimental validation, Int. J. Heat Mass Transf. 114 (2017) 169–186. https://doi.org/10.1016/j.ijheatmasstransfer.2017.06.063.

[18] L. Shen, Z. Tu, Q. Hu, C. Tao, H. Chen, The optimization design and parametric study of thermoelectric radiant cooling and heating panel, Appl. Therm. Eng. 112 (2017) 688–697. https://doi.org/10.1016/j.applthermaleng.2016.10.094.

[19] M. Mosa, M. Labat, S. Lorente, Role of flow architectures on the design of radiant cooling panels, a constructal approach, Appl. Therm. Eng. 150 (2019) 1345–1352. https://doi.org/10.1016/j.applthermaleng.2018.12.107.

[20] N. Arslanoglu, A. Yigit, Experimental and theoretical investigation of the effect of radiation heat flux on human thermal comfort, Energy Build. 113 (2016) 23–29. https://doi.org/10.1016/j.enbuild.2015.12.039.

[21] B. Ning, Y. Chen, H. Liu, S. Zhang, Cooling capacity improvement for a radiant ceiling panel with uniform surface temperature distribution, Build. Environ. 102 (2016) 64–72. https://doi.org/10.1016/j.buildenv.2016.03.009.

[22] R. Albatici, F. Passerini, A.M. Tonelli, S. Gialanella, Assessment of the thermal emissivity value of building materials using an infrared thermovision technique emissometer, Energy Build. 66 (2013) 33–40. https://doi.org/10.1016/j.enbuild.2013.07.004.

[23] J.R. Ehlert, T.F. Smith, View Factors for Perpendicular and Parallel, Rectangular Plates, J. Thermophys. Heat Transf. 7 (1993) 173–174.

[24] R.P. Chopade, S.C. Mishra, P. Mahanta, S. Maruyama, A. Komiya, Uniform thermal conditions on 3-D object: Optimal power estimation of panel heaters in a 3-D radiant enclosure, Int. J. Therm. Sci. 51 (2012) 63–76. https://doi.org/10.1016/j.ijthermalsci.2011.08.007.

[25] Y. Xin, W. Cui, J. Zeng, Experimental study on thermal comfort in a confined sleeping environment heating with capillary radiation panel, Energy Build. 205 (2019) 109540. https://doi.org/10.1016/j.enbuild.2019.109540.

[26] J. Dreo, A. Petrowski, E. Taillard, Métaheuristiques pour l'optimisation difficile, EYROLLES, 2003.

[27] H.-G. Beyer, H.-P. Schwefel, Evolution strategies–A comprehensive introduction, Nat. Comput. 1 (2002) 3–52.

[28] L. Gosselin, M. Tye-Gingras, F. Mathieu-Potvin, Review of utilization of genetic algorithms in heat transfer problems, Int. J. Heat Mass Transf. 52 (2009) 2169–2188. https://doi.org/10.1016/j.ijheatmasstransfer.2008.11.015.

[29] M. Haratian, M. Amidpour, A. asghar Hamidi, Conceptual development of constructal theory towards optimum sizing of radiant enclosures, Int. J. Therm. Sci. 137 (2019) 337–342. https://doi.org/10.1016/j.ijthermalsci.2018.11.014.

[30] M. Hamdy, A.-T. Nguyen, J.L.M. Hensen, A performance comparison of multi-objective optimization algorithms for solving nearly-zero-energy-building design problems, Energy Build. 121 (2016) 57–71. https://doi.org/10.1016/j.enbuild.2016.03.035.